ELSEVIER

Creep resistance of PI/SiO$_2$ hybrid thin films under constant and fatigue loading

Z.D. Wang *, X.X. Zhao

Institute of Engineering Mechanics, School of Civil Engineering, Beijing JiaoTong University, Beijing 100044, China

Abstract

This paper presents an experimental study on creep resistance of PI/SiO$_2$ hybrid thin films with silica-fillers weight varying in the range of 0–8%. Creep deformation, creep rate and creep compliance are utilized to evaluate the thin films' characteristics under constant stress (creep) and tension–tension fatigue tests. The effects of silica doping level, stress amplitude and force pattern (constant or sinusoidal) are also analyzed in the experiments. The results show that the existence of nano-silica can improve the creep resistance both under constant and fatigue loading. Compared with constant loading, fatigue loading can accelerate the creep deformation and creep rate, and significantly increase the creep compliance of PI/SiO$_2$ hybrid thin films in the primary creep stage. As the creep develops into the secondary stage, the stress amplitude will replace the stress pattern and play a dominated role, which is due to the different deformation mechanisms in different creep stages.
© 2007 Elsevier Ltd. All rights reserved.

Keywords: PI/SiO$_2$; B. Creep; B. Fatigue

1. Introduction

Polyimides (PIs) are considered to be one of the most important engineering materials because of their superior mechanical properties shown at different temperatures [1–3]. Since 1960s, essentially the beginning of the search for high temperature polymers, much attention has been paid on PIs than any other high performance polymers. Extensive application researches have demonstrated the possibilities to use PIs as buffer coatings, passivation layers, alpha particle barriers, interlayer dielectrics, water scale packages, etc. [4,5]. To further decrease their coefficient of thermal expansion (CTE) to match inorganic or metallic substrates and enhance their mechanical properties (e.g. fracture toughness), different kinds of nano-additives [6–8] have been introduced as reinforcements to construct nano-inorganic/PI composites.

Similar as other viscoelastic materials, PIs tend to exhibit time-dependent deformations (even damage) over a wide range of temperatures, which are defined by creep for a constant load. If a sinusoidal force pattern (dynamic load) is applied, the strain increase can be referred to as 'dynamic creep'. Creep deformation is a big barrier for thermoplastics to satisfy the requirements in long-term loading service because the accumulated strain might exceed the material's deformation limitation and lead to creep fracture of the structures. Hence it is of great importance to know about the creep properties and improve the creep resistance for thermoplastics and their composites.

In the past 10 years, a variety of inorganic nano-fillers have been considered as the reinforcements to improve the creep resistance of polymer matrix because they have high surface to volume ratio and the possibility of forming network structure by dispersing nano-fillers dispersed into polymer matrix to restrict the mobility of polymer chain [9]. Pegorettie et al. [10] researched the creep performance of recycled polyethylene terephthalate (PET) filled with layered silicate. They obtained a slight decrease of creep

---

* Corresponding author. Tel.: +86 10 51684070; fax: +86 10 516842094.
E-mail address: zhdwang@center.njtu.edu.cn (Z.D. Wang).

compliance and no-rising creep rate in composites than in pure matrix. Fornes and Paul [11] reported how to improve the glass transition temperature (T_g) of nylon 66 by introducing nano-particles to restrict the motion of the polymer chains. Ranade et al. [12] studied polyethylene/montmorillonite layered silicate (PE/MLS) films and found that the presence of rigid MLS contributed to the improved creep resistance of composites. Zhang and Yang [13,14] gave a general report about the creep resistance of polyamide 66 modified by different nano-fillers. In addition, some theoretical works were also carried out to predict the long-term creep behavior of nano-filler/polymer composites based on the short-term experimental data [15–17].

However, the above researches about the creep behaviors of nano-filler/polymer composite have been focused on static loading, with few reports involved in the dynamic creep resistance, especially the lack of comparison about the creep resistance difference between static and dynamic loading. The aim of this work is to present a general understanding of the creep behaviors of PI/SiO$_2$ nanocomposite thin films under constant and fatigue loading. The effects of silica doping levels, stress amplitude and stress pattern (constant or sinusoidal) are also considered.

2. Experimental procedure

Four types of thin films: pure PI, PI/SiO$_2$ hybrid thin films with 1, 3 and 8 wt.% silica doping levels, were prepared by an improved sol–gel technique. The average thickness of films is about 0.035 mm. Compared with the traditional processing technique, the new process can lead to a smaller particle size. More information about the processing technique and the static mechanical properties (tensile strength, Young's modulus, elongation at break and CTE) has been reported in Ref. [18]. For the fatigue experiment, an INSTRON digital micro-electromagnetism testing system was used which has a dynamic capacity of 10 N, maximum displacement of 2.5 mm, and maximum frequency of 50 Hz. A sinusoidal force oscillation at 10 Hz was applied for the experiments with a stress ratio $R = 0.1$ (minimum stress divided by maximum stress). For the static creep experiment, a constant loading rate of 1 N/s was carried out until the load (or stress) reached a pre-setting value, and then the stress value was kept as constant. The testing temperature for static and fatigue loading was maintained at about 298 K.

3. Experimental result and discussion

3.1. Hysteresis loop

In this study, the 'dynamic creep' was investigated by monitoring the change of hysteresis loops during fatigue process, by which different properties can be determined simultaneously, e.g. cyclic softening/hardening, stored and lost energies, material damping and cyclic creep behavior [19,20]. Fig. 1 presents typical hysteresis loops of pure PI and PI/SiO$_2$ hybrid thin films in different cyclic stages. The fatigue life (N_f) and cyclic number (N) are also presented in the figures, and the stress amplitude can be referred in Y-axis. As a comparison, the corresponding parts of stress–strain curves under quasi-static tensile loading are also plotted in Fig. 1. Like most of polymers and matrix-dominated polymeric composite to be viscoelastic, a significant phase lag of the strain to stress was exhibited under fatigue loading, which caused the formation of hysteresis loops even if the applied stress was much lower than the yield stress of materials. The area enclosed in the hysteresis loop denoted the specific mechanic energy (in per volume) dissipated in every cycle, which is partly converted into the heat energy and partly stored as deformation energy leading to the final failure of materials [21]. Table 1 lists the values of the specific energy (w_f) dissipated in the hystersis loops as shown in Fig. 1.

According to Fig. 1 and Table 1, the specific cyclic energy dissipated in every cycle is decreased with increasing fatigue cycles, which indicates the expending of the viscous resistance during the fatigue process. Another noteworthy point in Fig. 1 is that the increase of the minimum strain in hysteresis loops is much quicker than that of the maximum strain. The phenomenon of cyclic hardening is exhibited for the thin films, although it is inferred in some earlier review papers [22–24] that the mechanism of cyclic softening (e.g. large scale bulk flow of polymers under fatigue loading) commonly overwhelms that of cyclic hardening (e.g. the molecular orientation hardening and defect-hardening) for polymers under fatigue loading. The more prominent cyclic hardening in pure PI thin films compared to other hybrid films in Fig. 1 indicates that it is not caused by the presence of nano-silica particles.

Similar as the pure PI thin film, the areas enclosed in hystersis loops for PI/SiO$_2$ hybrid thin films doped with 1 and 3 wt.% silica contents also have a quick decrease during the primary stage, corresponding to the normalized fatigue life (fatigue cycle divided by the fatigue life) to be lower than 0.1. In addition, by introducing nano-silica particles with 1 and 3 wt.% doping levels, both the deformation resistance and the fatigue life are improved comparing with that of pure PI thin films. However, the fatigue loading capability or fatigue life is largely decreased as increasing the silica doping level up to 8 wt.%, although the fatigue deformation resistance keeps improving. For PI/SiO$_2$ hybrid thin films with 8 wt.% silica doping level, a much lower stress level was applied to realize a comparable cyclic number as that of other cases under the stress-controlled condition as shown in Fig. 1. Therefore, too higher silica doping level seems to impair the fatigue property of PI/SiO$_2$ hybrid thin films regardless the improvement of the creep resistance.

3.2. Creep strain and creep rate

The strain of a viscoelastic material is a time-dependent function and can be expressed by
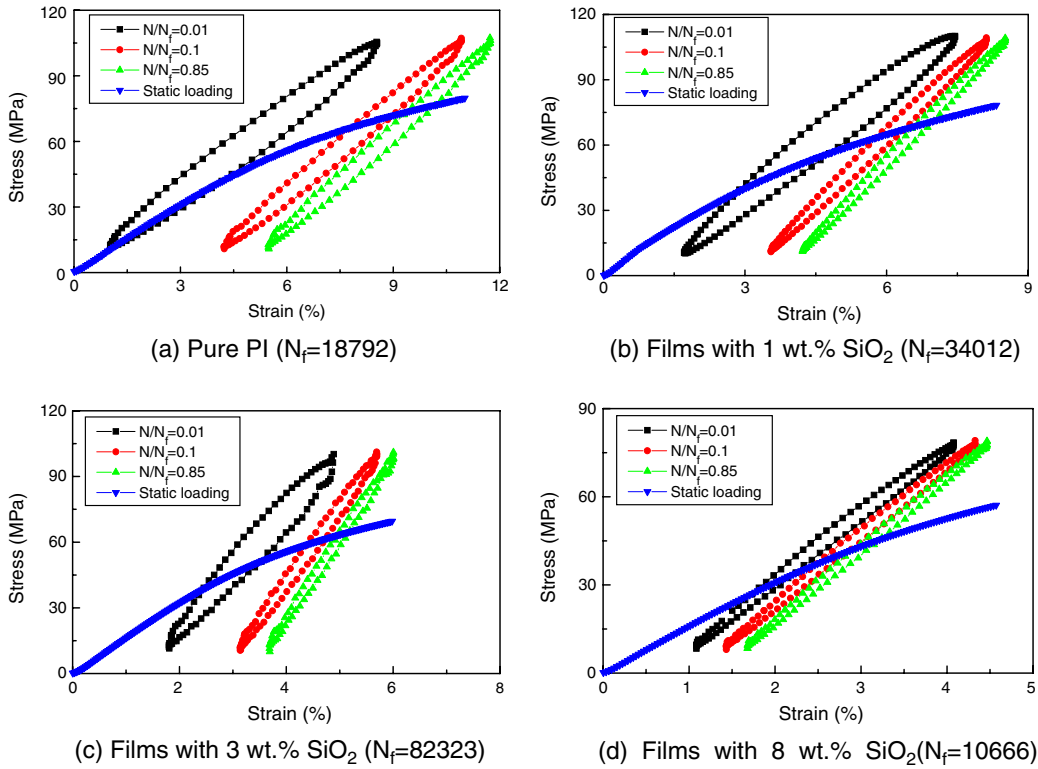
(a) Pure PI (N_f=18792)

(b) Films with 1 wt.% SiO$_2$ (N_f=34012)

(c) Films with 3 wt.% SiO$_2$ (N_f=82323)

(d) Films with 8 wt.% SiO$_2$(N_f=10666)

Fig. 1. Typical hysteresis loops for pure PI and PI/SiO$_2$ thin films (N and N_f denote cyclic number and fatigue life, respectively).

Table 1
Specific energy dissipated due to hysteresis loops

Sample	w_f (×10^4 J/m^3)		
	$N/N_f = 0.01$	$N/N_f = 0.1$	$N/N_f = 0.85$
Pure PI	100.3	58.8	46.2
1 wt.% SiO$_2$	83.1	31.4	22.7
3 wt.% SiO$_2$	44.2	19.1	13.3
8 wt.% SiO$_2$	11.2	10.5	8.56

$$\varepsilon = f(\sigma, t) \tag{1}$$

Fig. 2 shows the four stages of the deformation for polymers in the entire creep process schematically. (I) Instantaneous strain (ε_0), which is due to the elastic or plastic deformation of the crystallized polymer or regular chain once the external load is applied, and this stage is time-independent. (II) Primary creep strain (ε_1), which is resulted from the elastic deformation and viscous or orientated flow of amorphous polymer chains in short-term. (III) Secondary creep strain (ε_2), which is a long-time steady deformation and commonly considered to be associated with the damage from crystallized polymer or oriented non-crystalline regions. (IV) Tertiary creep strain (ε_3), which corresponds to the final creep rupture or advanced necking.

According to the result shown in Fig. 1, a significant creep deformation was exhibited in both pure PI and PI/SiO$_2$ hybrid thin films under fatigue loading, despite being partly decreased by increasing nano-silica additives. In
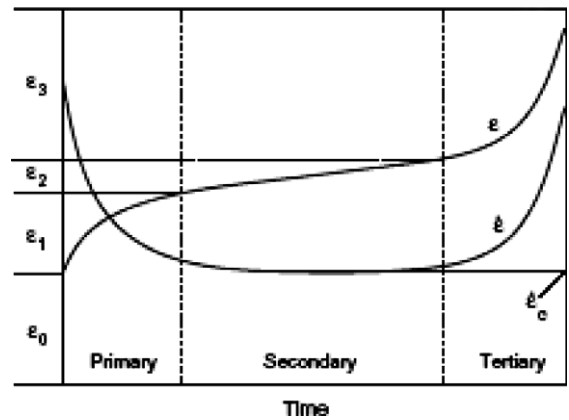

Fig. 2. Schematical creep stages by strain and strain rate [14].

order to give a comparison of the creep resistance and deformation behavior of PI/SiO$_2$ hybrid thin films under static and fatigue loading, static creep experiments were also conducted and the results are shown in Fig. 3. For the static experiments, different stress levels were applied in order to be comparable with the fatigue results, but the creep rupture or failure is not considered and the maximum creep time is only 10,800 seconds, which has been enough to be compared with the fatigue loading time. Therefore, the deformations were divided into instantaneous deformation, primary and unfinished secondary creep processes, and the tertiary stage was, however, not observed.
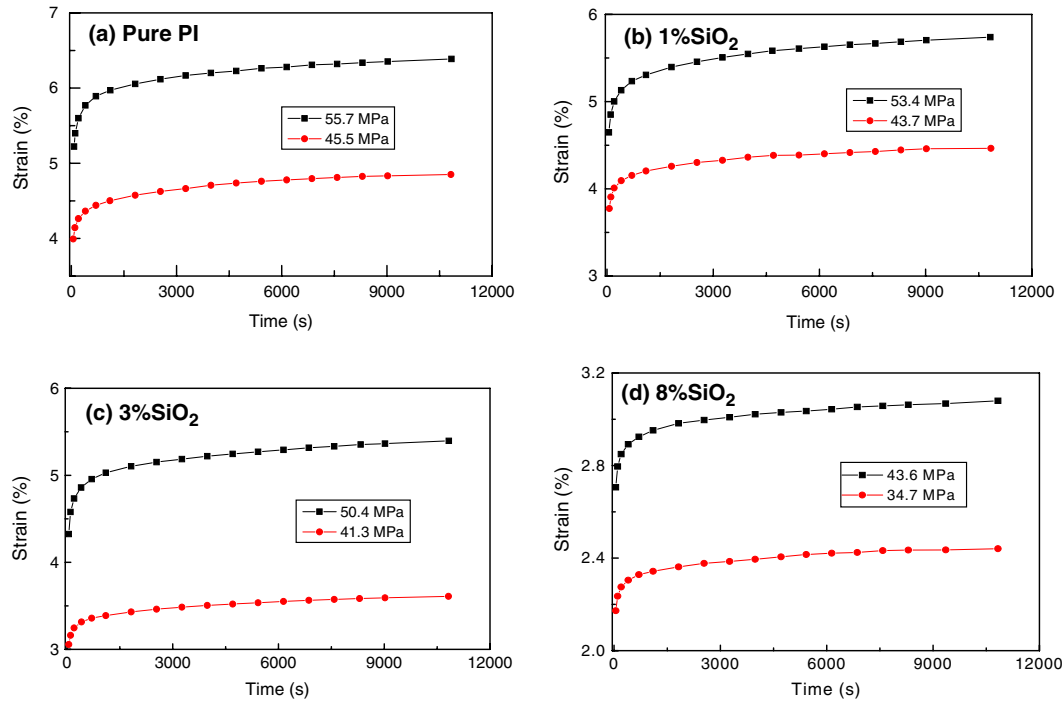
Fig. 3. Creep strain of pure PI and PI/SiO$_2$ thin films under static loading.

The experimental results in Fig. 3 clearly show that the deformation of PI/SiO$_2$ hybrid thin films is noticeably smaller than that of pure PI, and the creep resistance can be improved by increasing the silica-fillers under different stress levels applied. However, it does not increase linearly. For example, there is no significant difference between the results of the films with 1 wt.% and 3 wt.% silica doping levels, but the creep strain decreases remarkably when increasing silica-fillers up to 8 wt.%.

Fig. 4 provides the comparison of creep strains in pure PI and PI/SiO$_2$ hybrid thin films under static and fatigue loading. For the fatigue experiment, the creep strain is determined based on the average strain (or mean strain) of every hysteresis loop considering the different increasing rates of maximum and minimum strains in every hysteresis loop. The fatigue time is calculated by using the fatigue cycles divided by a factor of 10, due to the applied sinusoidal frequency 10 Hz. It is interesting to see that a nearly linear relationship is exhibited in the $\varepsilon \sim \log t$ coordinates for static loading, and no detectable transition can be found with the creep developing process from primary to secondary stage. The transition can be accurately simulated by Findley power law as [25]

$$\varepsilon_F = \varepsilon_{F0} + \varepsilon_{F1} t^n \tag{2}$$

However, the increase of the primary creep strain under fatigue loading is much quicker and significantly different from the linear relationship for pure PI and PI/SiO$_2$ hybrid thin films with 1 and 3 wt.% silica doping levels. The only exception is the 8 wt.% silica doping level, which might be caused by a too high silica doping level decreasing the vis-

coelastic property of materials (c.f. hysteresis loop as shown in Fig. 1). During the secondary stable creep stage, the creep rate of fatigue loading is also higher than that of the static loading, but it is not as remarkable as that in the primary stage. Moreover, the tertiary creep stage (creep softening) was not observed in this study, excepting the case of the hybrid thin film with 8 wt.% silica doping level under the fatigue stress of 28.8 ± 24.4 MPa. Therefore, it is reasonable to believe that the final creep failure for polymeric and their hybrid thin films might be abrupt and unpredicted, which is much different from their bulk materials.

In addition to creep deformation, the dimensional stability of materials is also described by another important parameter named creep rate, which defines the velocity of the creep deformation and is calculated by the slope of creep strain versus loading time. According to the results shown in Fig. 4, the creep rate can be improved with increasing the applied stress or adopting fatigue loading. The creep rates of pure PI and PI/SiO$_2$ hybrid thin films with different silica doping levels under static and fatigue loading are shown in Fig. 5. It is noticeable that the creep rate started at a much higher level for fatigue loading, then it decreased very quickly comparing with that of the static loading (c.f. the primary creep time of the static loading as shown in Fig. 3). It also shows that the creep rate could be significantly decreased by increasing the silica doping levels.

The creep rate in the second creep stage nearly keeps as a constant value, so the average creep rate $\dot{\varepsilon}_{II}$ can be used to determine the material performance in this stage. The complete results are listed in Table 2. Fig. 6 provides a repre-
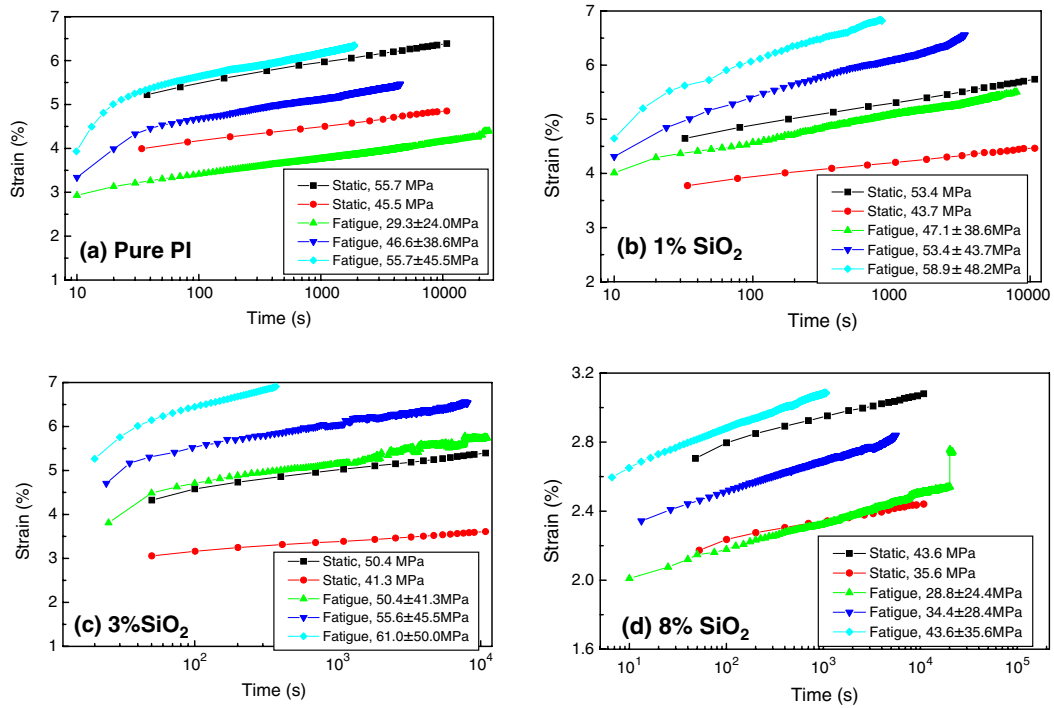
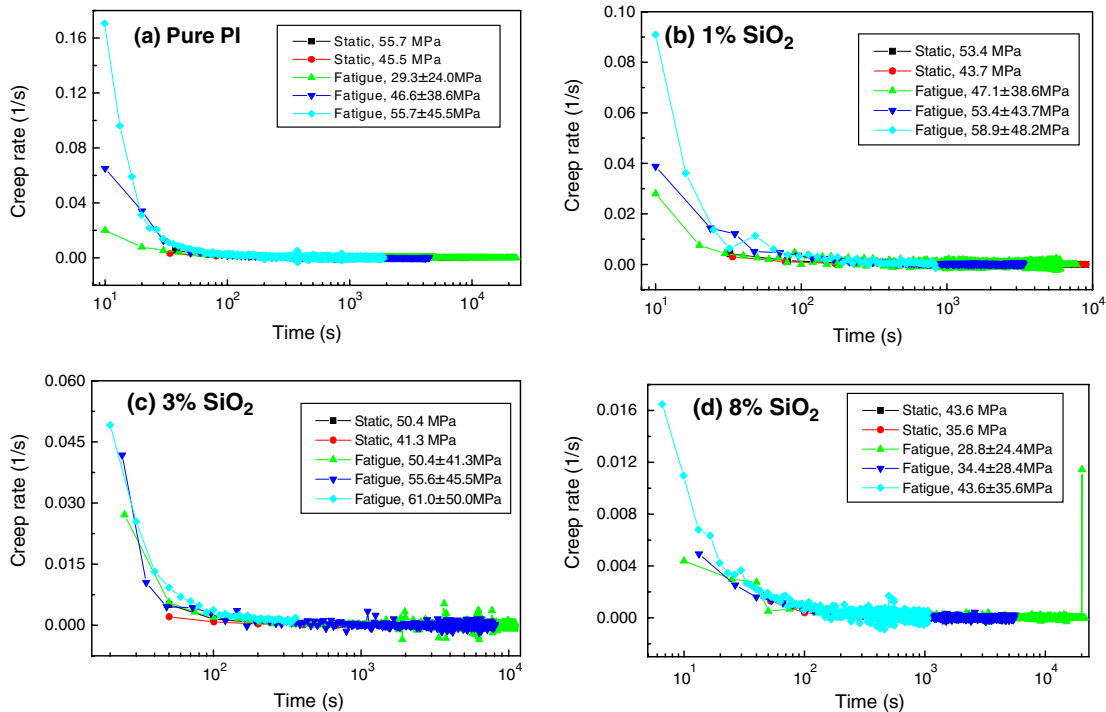Fig. 4. Comparison of creep strains of pure PI and PI/SiO$_2$ thin films under static and fatigue loading.

Fig. 5. Creep rate of pure PI and PI/SiO$_2$ thin films under constant and fatigue loading.

sentative comparison of $\dot{\varepsilon}_{II}$ among pure PI and PI/SiO$_2$ hybrid thin films with different silica doping levels under static loading. Although the applied stresses are slightly different in Fig. 6, the results clearly show that the creep rate can be significantly reduced by increasing the silica doping levels. According to the result listed in Table 2, the average creep rate $\dot{\varepsilon}_{II}$ is significantly accelerated by fatigue loading instead of static loading. Compared with that

Table 2
Average creep rate $\dot{\varepsilon}_{II}$ affected by silica-fillers and stress levels

Sample	Stress (MPa)	$\dot{\varepsilon}_{II}(\times 10^{-5}\ s^{-1})$
Pure PI	55.7	5.13
	45.5	3.58
	55.7 ± 45.5	28.65
	46.6 ± 38.6	9.97
	29.3 ± 24.0	2.18
1 wt.% SiO$_2$	53.4	4.28
	43.7	2.79
	58.9 ± 48.2	83.46
	53.4 ± 43.7	20.40
	43.1 ± 38.6	5.43
3 wt.% SiO$_2$	50.4	3.61
	41.3	2.24
	61.0 ± 50.0	141.46
	55.6 ± 45.5	15.84
	50.4 ± 41.3	6.30
8 wt.% SiO$_2$	43.6	1.13
	35.6	1.00
	43.6 ± 35.6	18.24
	34.0 ± 28.4	3.12
	28.8 ± 24.4	0.81

Table 3
Empirical constants of the creep compliance simulated by Findley power law

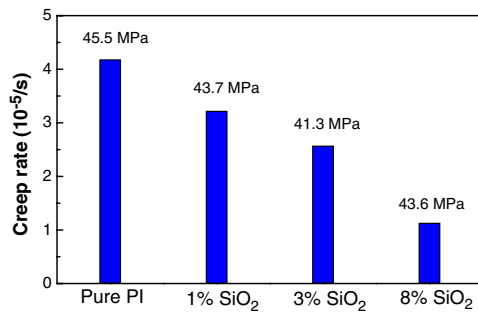| Sample	Stress (MPa)	S_0 (GPa^{-1})	S_F (GPa^{-1})	n
Pure PI	55.7	0.860	0.069	0.155
	45.5	0.831	0.057	0.152
	55.7 ± 45.5	0.738	0.104	0.165
	46.6 ± 38.6	0.762	0.113	0.163
	29.3 ± 24.0	0.922	0.120	0.151
1 wt.% SiO$_2$	53.4	0.809	0.061	0.156
	43.7	0.805	0.051	0.157
	58.9 ± 48.2	0.761	0.129	0.163
	53.4 ± 43.7	0.787	0.112	0.158
	43.1 ± 38.6	0.884	0.090	0.155
3 wt.% SiO$_2$	50.4	0.807	0.054	0.159
	41.3	0.801	0.053	0.155
	61.0 ± 50.0	0.769	0.114	0.167
	55.6 ± 45.5	0.775	0.069	0.163
	50.4 ± 41.3	0.732	0.068	0.161
8 wt.% SiO$_2$	43.6	0.585	0.033	0.144
	35.6	0.587	0.031	0.142
	43.6 ± 35.6	0.550	0.057	0.150
	34.0 ± 28.4	0.647	0.052	0.149
	28.8 ± 24.4	0.691	0.045	0.141

Fig. 6. Comparison of $\dot{\varepsilon}_{II}$ among pure PI and PI/SiO$_2$ thin films under static loading (the loading stresses are shown simultaneously).

of the stress pattern, the effect of silica-fillers is very limited although its existence can partly decrease the average creep rate $\dot{\varepsilon}_{II}$.

3.3. Creep compliance

Similar as the creep strain and creep rate, creep compliance, $S(\sigma,t)$, is also frequently applied to describe the creep performance and is defined by

$$S(\sigma,t) = \frac{\varepsilon(\sigma,t)}{\sigma} \tag{3}$$

Substituting Eq. (1) into Eq. (3), the creep compliance simulated by Findley power law can be expressed as

$$S(t) = \frac{\varepsilon(\sigma,t)}{\sigma} = S_0 + S_1 t^n \tag{4}$$

The values of the empirical constants S_0, S_1 and n defined in Eq. (4) are listed in Table 3. In contrast to the creep

strain and strain rate, creep compliance $S(\sigma,t)$ has been normalized by the applied stress. Therefore, it provides a possibility to compare the creep data from different tests at different stress levels. Fig. 7 presents the testing results of the creep compliance for pure PI and PI/SiO$_2$ hybrid thin films under static and fatigue loading. In this study, the creep compliance under fatigue loading is determined by the creep strain divided by the average stress in every hysteresis loop. According to the results shown in Fig. 7, it seems that the fatigue creep compliance is much higher than the static creep compliance, which is understandable. The tension–tension fatigue stress can be regarded as a mean stress overlapped by a sinusoidal various stress, and the various stress will definitely accelerate the creep deformation and improve the creep compliance. Because the fatigue creep compliance in Fig. 7 is only determined by the mean stress and the effect caused by the sinusoidal various stress is neglected, the results are naturally lower than that received by static loading.

It is also worth to point out that the creep compliances are reduced when increasing the applied stress both under fatigue and static loading, which are due to the non-linear deformation of polymers. In addition, the difference of the creep compliance under different stress levels is also getting smaller by increasing the silica doping levels. For constant loading, the difference of the creep compliance is less than 10% under the different stress levels in pure PI and PI/SiO$_2$ composite films with 1% and 3% silica doping levels. As the silica doping level increases to 8 wt.%, There is no noticeable change of the creep compliance, which indicates that the linear-elastic response will become more evident when increasing the silica doping levels. Comparatively, the results of the fatigue loading are more irregular.
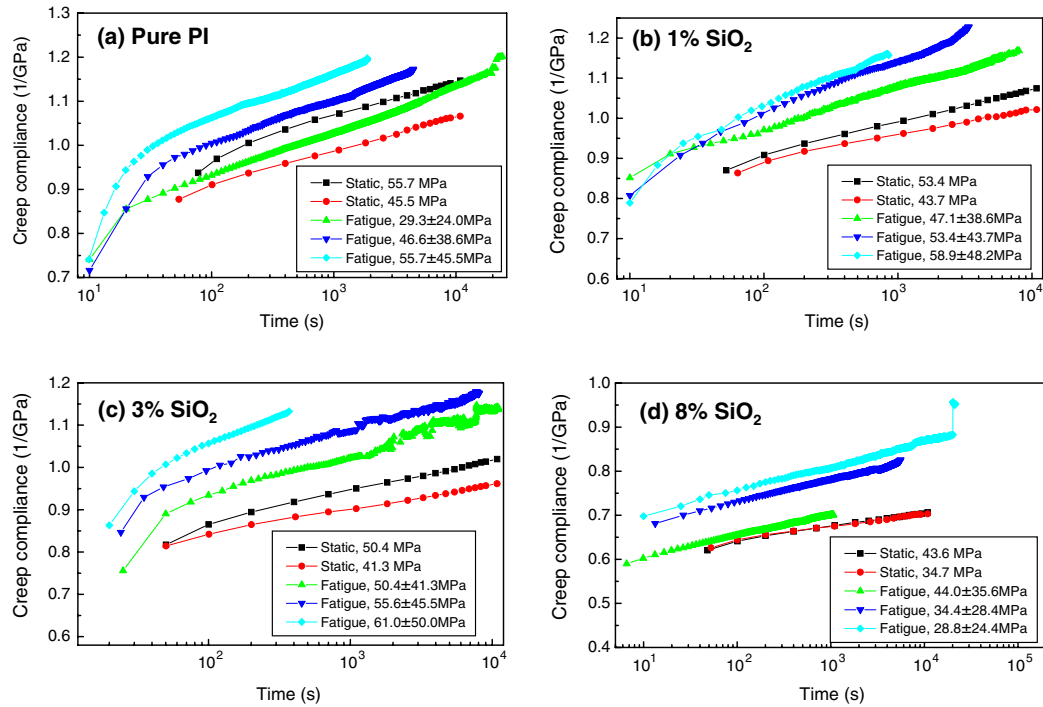
Fig. 7. Creep compliance of pure PI and PI/SiO$_2$ thin films under static and fatigue loading.

3.4. Structure-property analysis

PI can be regarded as the constitution of crystallized and amorphous regions in micro-structure as other semicrystalline polymers. The response of the crystallized region to external load is instantaneous and elastic, and it is time-dependent and viscoelastic in the amorphous region. Since the crystallized chains are comparatively fixed and the amorphous chains are mobile, the additive of nano-silica particles are mainly located in the amorphous regions, partly agglomerated and partly uniformly dispersed.

Once an external load is applied, the crystallized chains would show an elastic response immediately. Because the deformation and viscous flow are time-dependent in the amorphous regions, their contributions to the instantaneous deformation of specimens and the creep compliance are limited. Similarly, because the nano-silica particles are mainly located in the amorphous region [18], particle-fillers can only slightly improve Young's modulus and instantaneous deformation resistance of materials.

During the primary creep stage, the deformation is major induced by the viscous flow of amorphous chains. This kind of viscous flow is strongly time-dependent and will be decreased quickly with increasing the loading time. Therefore, the area enclosed in the hystersis loop of PI/SiO$_2$ composite films is remarkably reduced at the initial fatigue process as shown in Fig. 1. Generally, it is believed that a huge number of nano-particles dispersed in the amorphous region can form a network [26], which cooperates with the amorphous chains via inter-phase, bridging segments and junctions to bear load and restrict the immo-

bility of the amorphous chains. Therefore, the viscoelastic behavior of materials can be significantly deceased with increasing the silica doping level which is different from Young's modulus of materials, and the primary creep rate is also greatly reduced by the existence of the silica-fillers as shown in Fig. 5. In addition, the experimental results show that the primary creep rate is greatly enhanced by applying the fatigue load instead of a constant load, because the fatigue load can accelerate the viscous flow of the amorphous chains as comparing with the constant load. About the effect of the stress amplitude, it is natural that higher stress level will accelerate the viscous flow of the amorphous chains and increase the primary creep rate of materials. However, the experimental results show that the effect of the stress level is not as remarkable as that of the stress pattern (fatigue loading instead of constant loading).

Different from the recoverable primary creep deformation coming from the viscous flow of the amorphous chains, the deformation of the secondary creep stage is mainly associated with the damage of crystallized polymer and oriented non-crystalline regions, such as the pulling out of chain folds by a crystal slip process and the breaking of an inter-crystalline tie molecule, and the irreversible deformation from amorphous regions, such as the breaking of bridging segments, disengaged junction between fillers and polymer chains and the pulling out of a chain entanglement [15]. Therefore, the deformation during this stage is irreversible.

Similar as that of the primary creep stage, the creep strain, creep rate and creep compliance in the secondary stage are accelerated by improving the stress level or

'applying fatigue load, and decreased by increasing the silica doping levels. However, due to the completely different deformation mechanisms existed in these two stages, different intrinsic characteristics are exhibited in the experimental results. For example, Fig. 5 shows that the primary creep rate under fatigue loading is generally much higher than that under constant loading regardless the different stress levels applied, which indicates that the stress pattern has the most important role in accelerating the viscous flow of the amorphous region. However, as the creep develops into the secondary stage, the testing results listed in Table 2 show that the stress level will replace the stress pattern to play the dominated role.

As we consider the secondary creep to be associated with the damage of crystallized and amorphous chains, the results become easily to be understandable. It is known that each material has its own static strength and fatigue limit. If the applied stress is lower than the static strength or fatigue limit of the material, no damage happens. Naturally, it is reasonable to believe that the crystallized and amorphous chains in semicrystalline polymers also have their individual static strength and fatigue limits. Considering the inhomogeneous distributions in all crystallized and amorphous chains, only a few poor chains might be damaged if the applied stress is much lower than the average static strength or fatigue limit of the crystallized and amorphous chains. As the applied stress exceeds the critical values, the damage will take place in most chains, and a higher creep rate will be received. Therefore, different from the primary creep stage, the secondary creep stage is significant affected by the stress amplitude other than the stress pattern.

4. Conclusions

The creep experiments of PI/SiO$_2$ nanocomposite films are carried out under static and fatigue loading. Creep stain, creep rate and creep compliance are obtained under different stress levels and different stress patterns. The experimental results exhibits significant cyclic hardening in pure PI and PI/SiO$_2$ composite films under fatigue loading. The phenomena of the energy dissipation, cyclic creep and cyclic hardening are mainly happened on the initial stage, corresponding to the cyclic number to be lower than about 0.1 of the fatigue life of the materials.

About the creep deformation, the results show that the primary creep stage is associated with the viscous flow of the amorphous chains and the stress pattern works as a dominated role than other factors. As the creep developed to the secondary stage, it is the stress level instead of the stress pattern which plays a dominated role because the necessary stress level must be reached to lead final damage of crystallized and amorphous chains.

In addition, the results showed that the suitable silica contents can effectively improve the creep resistance and fatigue life of PI/SiO$_2$ composite films. However, as the silica doping level increased to 8 wt.%, the fatigue life of

materials is significantly decreased although the creep resistance keeps a further improvement. Therefore, in order to improve the performance of this class of nanocomposites and make them suitable for long-time loading applications in static and dynamic loading conditions, other factors (e.g. plastic deformation capability) should also be considered.

References

[1] Wilson D, Stenzenberger HD, Hergenrother PM, editors. Polyimides. Glasgow: Blackie; 1990.
[2] Volksen W, Hergenrother PM, editors. High performance polymers. Berlin: Springer; 1994.
[3] Yamaoka H, Miyata K, Yano O. Cryogenic properties of engineering plastic films. Cryogenics 1995;35:787–9.
[4] Ghosh KL, Mittal KL. Polyimides, fundamentals and applications. New York: Marcel Dekker; 1996.
[5] Mittal KL, editor. Polyimide; synthesis, characterization, and applications. New York: Plenum Press; 1993.
[6] Mark JE. Ceramic-reinforced polymer and polymer-modified ceramic. Polym Eng Sci 1996;36:2905–20.
[7] Ha CS, Cho WJ. Microstructure and interface in organic/inorganic hybrid composites. Polym Adv Technol 2000;11(3):145–50.
[8] Agag T, Koga T, Takeichi T. Studies on thermal and mechanical properties of polyimide-clay nanocomposites. Polymer 2001;42:3399–408.
[9] Brechet Y, Cavaille JYY, Chabert E, et al. Polymer based nanocomposites: Effect of filler–filler and filler–matrix interactions. Adv Eng Mater 2001;3:571–7.
[10] Pegoretti A, Kolarik J, Peroni C, et al. Recycles poly(ethylene terephthalate)/layered silicate nanocomposites: morphology and tensile mechanical properties. Polymer 2004;45:2751–9.
[11] Fornes TD, Paul DR. Crystallization behavior of nylon 6 nanocomposites. Polymer 2003;44:3945–61.
[12] Ranade A, Nayak K, Fairbrother D, et al. Maleated and non-meleated polyethylene-montmorillonite layered silicate blown films: creep, dispersion and crystallinity. Polymer 2005;46:7323–33.
[13] Zhang Z, Yang JL, Friedrich K. Creep resistant polymeric nanocomposites. Polymer 2004;45:3481–5.
[14] Yang JL, Zhang Z, Schlarb AK, Friedrich K. On the characterization of tensile creep resistance of polyamide 66 nanocomposites. Part I. Experimental results and general discussions. Polymer 2006;47:2791–801.
[15] Yang JL, Zhang Z, Schlarb AK, Friedrich K. On the characterization of tensile creep resistance of polyamide 66 nanocomposites. Part II: Modeling and prediction of long-term performance. Polymer 2006;47:6745–58.
[16] Sarvestani AS, Picu CR. Network model for the viscoelastic behavior of polymer nanocomposites. Polymer 2004;45:7779–90.
[17] Blackwell RI, Mauritz KA. Mechanical creep and recovery of poly(styrene-b-ethylene/butylene-b-styrene) (SEBS), sulfonated SEBS (sSEBS), and sSEBS/silicate nanostructured materials. Polym Adv Technol 2005;16:212–20.
[18] Wang ZD, Lu JJ, Li Y, et al. Low temperature properties of PI/SiO$_2$ nanocomposite films. Mater Sci Eng B 2005;123(3):216–21.
[19] Keller T, Tirelli T, Zhou A. Tensile fatigue performance of pultruded glass fiber reinforced polymer profiles. Compos Struct 2005;68:235–45.

[20] Fray ME, Altstadt V. Fatigue behaviour of multiblock thermoplastic elastomers. 2. Dynamic creep of poly(aliphatic/aromatic-ester) copolymers. Polymer 2003;44:4643–50.

[21] Ferry JD. Viscoelastic property of polymers. 2nd ed. New York: John Wiley and Sons; 1970.

[22] Manson JA, Hertzberg RW. Critical reviews in macromolecular. Science 1973;1:433–8.

[23] Rabinowitz S, Beardmore PJ. Cyclic deformation and fracture of polymers. Mater Res 1974;9:81–99.

[24] Sure JA, Richardson GC. Fatigue of polymers. Int J Fract 1980;16:499–516.

[25] Findley WN, Lai JS, Onaran K. Creep and relaxation of nonlinear viscoelastic materials: with an introduction to linear viscoelasticity. New York: Dover Publications, Inc; 1989.

[26] Brechet Y, Cavaille JYY, et al. Polymer based nanocomposites: Effect of filler–filler and filler–matrix interactions. Adv Eng Mater 2001;3:571–7.